Pressure Drop in Gas Slugs in Vertical Tubes and Flooding Instability

J. R. F. Guedes de Carvalho and M. J. F. Ferreira
Dep. de Engenharia Quimica, Faculdade de Engenharia da Universidade do Porto, 4050-123 Porto, Portugal

Fast-response differential-pressure transducers were used to continuously monitor the pressure difference between two nearby points along single gas slugs rising in long vertical tubes filled with liquid. Operating pressures in the 0.6 to 6.0-MPa range gave slugs of argon with densities in the 10 to 100-kg/m^3 range, rising through mixtures of glycerol and water with viscosities in the 10^{-3}- to 305×10^{-3}-Pa·s. range. The transducer records suggest that, for all the liquids tested, there was flooding instability of the film flowing around the slugs when the gas density was raised sufficiently. With the assumption that flooding instability is due to the force on the waves moving along the gas–liquid interface, dimensional analysis shows that the observations with gas slugs correlate well with flooding data obtained in wetted wall tubes operating at atmospheric pressure. The work reveals strong limitations of current empirical correlations for the prediction of flooding in wetted wall tubes.

Introduction

Gas slugs, or Taylor bubbles (see Figure 1a), form spontaneously in gas–liquid flow in long vertical tubes, in regions where the fractional gas holdup is high. In the present article we consider the particular type of gas slug that originates when a long tube, initially full of liquid, is held vertically with its top end sealed, while at its lower end the liquid is allowed to run down freely (see Figure 1b).

In low to moderate viscosity liquids, the velocity of rise of these slugs is given as

$$u_s = 0.35\,(gD)^{1/2}\gamma^{1/2}, \tag{1}$$

where g is the acceleration due to gravity, D is the tube diameter, and γ is the dimensionless ratio $(\rho - \rho_g)/\rho$, where ρ and ρ_g are the densities of liquid and gas, respectively. Equation 1 does not account for the effect of surface tension, which becomes relevant only when the tube diameter is small (Wallis, 1969). With increasing liquid viscosity, the point will come where Eq. 1 ceases to be valid and u_s becomes a decreasing function of liquid viscosity (Wallis, 1969), but it is usually a simple matter to measure u_s by timing the passage of the slug between two levels, which are a known distance apart.

Correspondence concerning this article should be addressed to J. R. F. Guedes de Carvalho.

At some distance down from the nose of the slug, the gas and liquid flow pattern will be indistinguishable from that observed in a wetted-wall column (see Figure 1c). As demonstrated by Nicklin et al. (1962), the liquid runs down the wall as a film of constant thickness, δ, while the gas flows up in the tube core, with average velocity u_s. The volumetric rate of gas flow up the tube core will be equal to the volumetric rate at which liquid runs down the wall,

$$q = \left(\frac{\pi}{4}\right)(D - 2\delta)^2 u_s, \tag{2}$$

because the tube is closed at the top.

In film flow along a wall, an important parameter is the volumetric rate of liquid flow per unit length of the wall perimeter, $Q = q/(\pi D)$, which in dimensionless form gives the Reynolds number for the falling film

$$Re = \frac{4Q}{\nu} = \frac{u_s(D - 2\delta)^2}{\nu D}, \tag{3}$$

where $\nu = \mu/\rho$ is the kinematic viscosity of the liquid; as detailed below the value of Re largely determines whether film flow is laminar or turbulent.

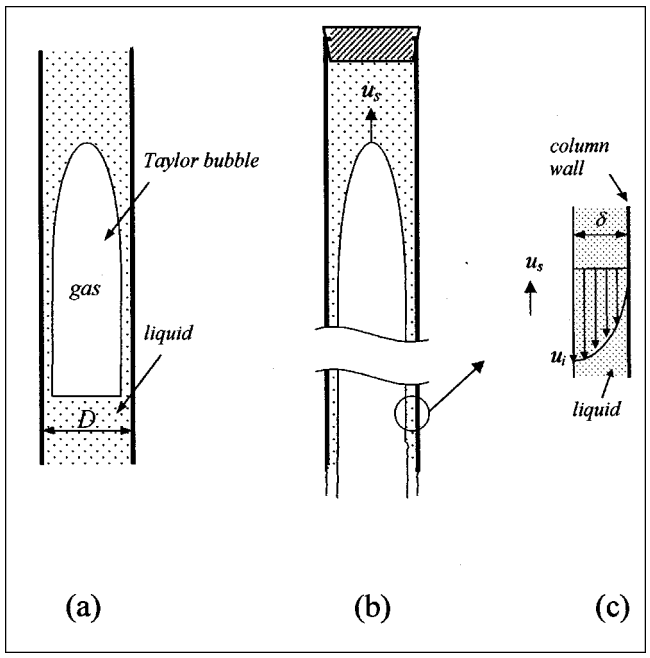

Figure 1. Gas slugs and detail of velocity profile.

In countercurrent annular flow in tubes, a condition known as flooding sets a limit for stable operation. This condition is conveniently described considering flow in a wetted-wall tube (see Figure 2), which is being fed with liquid at a constant flow rate Q (per unit length of wall perimeter). The liquid is introduced (Q_{in}) and removed (Q_{out}) through porous portions of the tube wall, and the pressure drop along the gas core, $\Delta P = P_B - P_A$, is followed by means of pressure gauges. If the superficial velocity of the gas, $U = u(D-2\delta)^2/D^2$, is varied over a wide range, it is possible to establish the dependence on U of both the pressure drop, ΔP, and the rate of liquid entrainment above the feed point, $W = (Q_{\text{in}} - Q_{\text{out}})\pi D$.

Experiments of this type have been reported by, among others, Hewitt and Wallis (1963), Hewitt et al. (1965), and Dukler et al. (1984), for air–water, and by Clift et al. (1966) for air–glycerol solutions.

Typical plots of ΔP vs. U and W vs. U are shown in Figure 2b, and according to Dukler et al. (1984), the inception of flooding, which is determined by the gas velocity above which W departs from zero, "coincides quite precisely with a steep increase in pressure gradient." According to the same authors, who used fast-response transducers to record the pressure at several locations along the flow tube, "the initiation of flooding is accompanied by a sharp increase in the level of fluctuation in pressure gradient as well as in its mean value." This will be seen as an important aspect in the interpretation of our experiments, reported below, but we will often use the expression flooding instability rather than flooding for reasons that will become apparent in due course.

The transition from orderly countercurrent annular flow (at low U) to the flooded condition (at high U) is clearly accompanied by a steep increase in the action exerted by the gas on the liquid, and it is instructive to consider the interfacial shear stress for the different flow conditions.

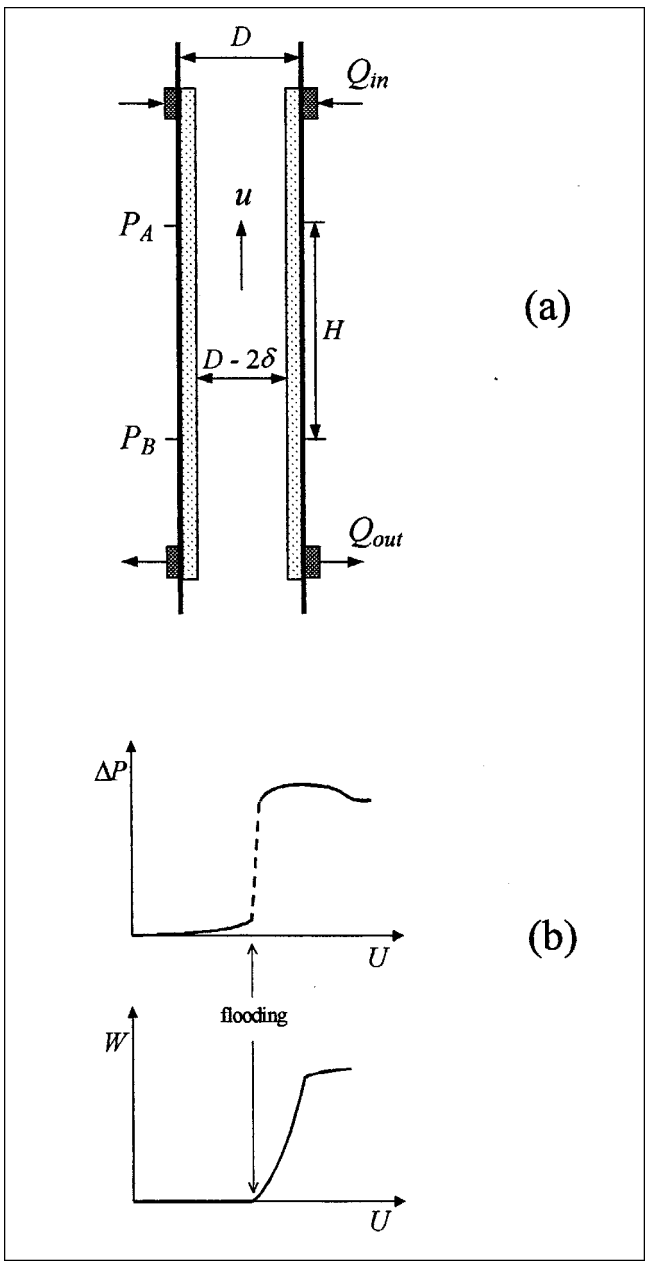

Figure 2. Experiment for determination of flooding velocity.

$\Delta P = P_B - P_A$; $U = u(D-2\delta)^2/D^2$ and $W = (Q_{\text{in}} - Q_{\text{out}})\pi D$.

If a force balance is performed on the flowing gas along a length H of the tube (see Figure 2a), it is possible to obtain

$$\tau_i = \frac{D-2\delta}{4}\frac{\Delta P_f}{H}, \tag{4}$$

where τ_i is the average shear stress across the interface and $\Delta P_f = P_B - P_A - \rho_g gH$ is the frictional pressure drop in the gas core. The contribution of the term $\rho_g gH$ is negligible at atmospheric pressure and it is therefore clear from the plot in Figure 2b that flooding is associated with a marked increase in the shear stress exerted by the gas on the liquid.

Hewitt et al. (1965) and Dukler et al. (1984) measured pressure gradients in wetted-wall flows in 32- and 51-mm-diameter tubes, respectively. Working at $Re < 1600$, Hewitt et al. (1965) observed that the pressure gradient before flooding never exceeded 90 N/m^3, and this limit is not far from that found by Dukler et al. (1984) for $Re \approx 2300$. Above the flooding point, pressure gradients of between 300 and 1000 N/m^3 were reported by both groups. In terms of interfacial shear stress, we would therefore expect values lower than 0.6–1.5 N/m^2 below the flooding limit, followed by a steep increase to about 3–8 N/m^2 at the transition point.

A closer analysis of the interaction between gas and liquid requires additional information on the mechanics of film flow down vertical walls, and this will be considered in another section.

In a wide range of studies reported in the literature [such as the reviews by McQuillan and Whalley (1985) and Bankoff and Lee (1981)] it has been found that, both with water and with viscous liquids, gas velocities of the order of 2–6 m/s are needed to reach the flooding point when working with air at (or near) atmospheric pressure. Equation 1 shows that u_s varies between 0.15 and 0.35 m/s when the tube diameter varies between 0.02 and 0.1 m, and therefore flooding is not expected to occur during the rise of single slugs in quiescent liquid at atmospheric pressure. Note that in cocurrent upward flow of gas and liquid, slugs rise with a velocity that can be much higher than is observed in quiescent liquids, and, following Nicklin and Davidson (1962), the possibility of flooding of the film around the slugs is an explanation for the slug/churn flow transition. If it is considered that flooding instability is the result of the force exerted by the gas on the liquid, its occurrence will be determined by the rate of momentum transfer between gas and liquid and, as a first approximation, this rate of momentum transfer may be assumed to be proportional to $\rho_g u_r^2$, where u_r is the relative velocity between gas and liquid. It is therefore to be expected that flooding velocities will be a decreasing function of gas density, and it can be conjectured that, by increasing the density of the gas, it will be possible to reach conditions of flooding instability with a single gas slug rising in a tube filled with liquid.

Our work program was designed to test this hypothesis, and it is important to start by giving a detailed description of the experimental method that we developed for that purpose.

Experimental Method

The basic features of the rig are illustrated in Figure 3, which shows a long and narrow tube standing vertically on top of a thick-walled reservoir, all in stainless steel. In our experiments we used two tube sizes: one was 21 mm ID × 3.15 m long, and the other 32.8 mm × 3.50 m. A large-bore ball valve (B) separated the tube from the reservoir and a conical adapter (with a small angle) was used to smoothly match the internal diameters of tube and valve. Valves A and F were initially closed, and before starting the experiments, valve B was closed and the column was completely filled with distilled water through valve C. The 1-mm-ID tubes connecting the column to the transducers were then completely filled with water from the column, making use of two "bleed screws," one on each side of the transducer membrane. With

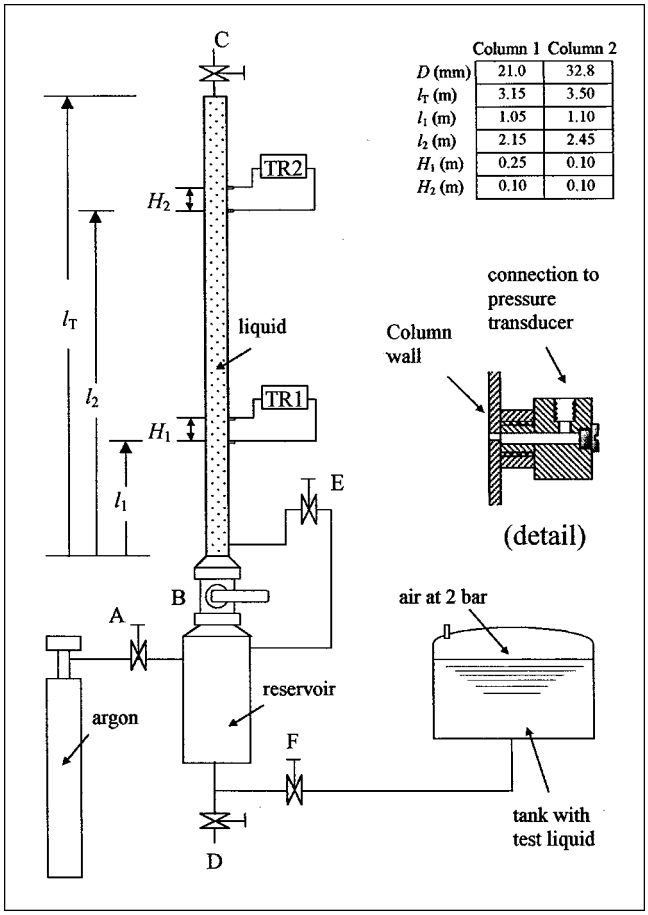

	Column 1	Column 2
D (mm)	21.0	32.8
l_T (m)	3.15	3.50
l_1 (m)	1.05	1.10
l_2 (m)	2.15	2.45
H_1 (m)	0.25	0.10
H_2 (m)	0.10	0.10

Figure 3. Rig with details of pressure tapping and connection to transducer.

these bleed screws tightly closed, the water in the column was emptied through B and D and air was blown downward through C for a short while, to help drag the water down the column wall (the reader should realize that the tubes connecting the transducer to the column remained full of water). Rinsing the column and reservoir with test liquid followed, and valve D was then closed while F was gradually opened until the column was filled to the top with liquid from the tank. Valves B and F were then closed and valve D opened to empty the liquid in the reservoir (the tube connecting the reservoir to A was temporarily loosened to let air in while the liquid drained through D). Valve E was then opened for a while until the liquid in the column started to fall back into the reservoir via E, leaving this bypass capillary full of test liquid. After closing valve E, the column was topped up with test liquid through C, following which this ball valve was closed. With valve F closed, argon was admitted to the reservoir through A and let out through D for a while to "wash away" the air initially present. After closing D, the pressure of argon in the reservoir was allowed to build up to the value (P) at which the experiment was to be performed, and valve A was then closed.

At this stage the column (between B and C) and the capillary connecting it to E were full of test liquid, at atmospheric pressure, while the reservoir was full of argon at the test pressure, P. Valve E was then opened slowly to equalize the

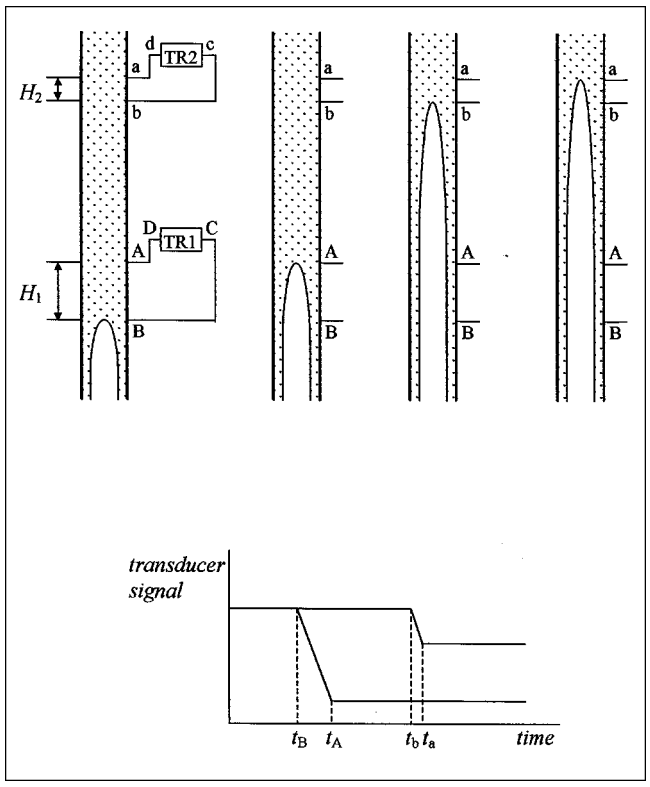

Figure 4. Slug rise and simplified transducer signal.

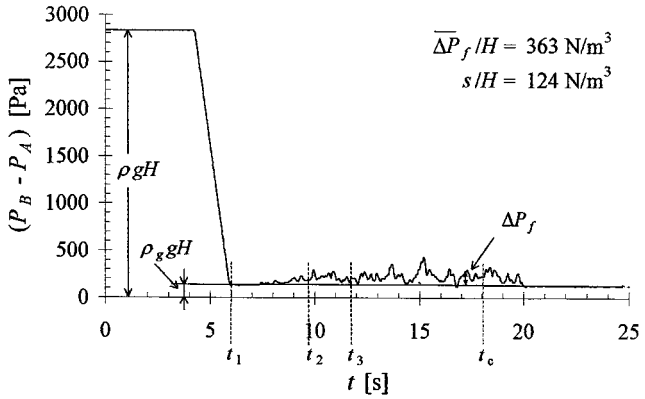

Figure 5. Detailed transducer signal.

Glycerol solution 1; P = 3.1 MPa; D = 21 mm.

pressure in the column with that in the reservoir, following which valve B was opened fully (with a quick stroke). At this stage the liquid started to drain along the tube wall into the reservoir, while the high-density gas rose along the core in the form of a slug, without any noticeable change in the value of the absolute pressure (P). This is because the system is closed and the solubility of argon in the liquid is very small. The slug rose at constant velocity, u_s, all the way up the column, until it stopped at C. Fast-response differential-pressure transducers, TR1 and TR2, were connected to the column at two different levels (see Figure 3) and their readings were recorded on a microcomputer at 100 Hz. The simplified signals corresponding to the rise of a long slug past the two transducers is sketched in Figure 4, where four instants are singled out for reference. The signals are simplified in that they only represent the variation in hydrostatic pressure between the probes, and the signals sketched are for slugs that are longer than the distance from the top of the column to the tappings of the pressure transducer. In the experiments performed initially in the 32.8-mm-ID tube, the reservoir did not have enough volume to collect all the liquid from the tube, and the resulting slugs were long but closed at the bottom, as in Figure 1a. In those instances, the signal of the pressure transducer would rise to the original base line, when the liquid again came to fill the space between the pressure tappings. Whatever the situation, the velocity of the slug may be obtained by dividing the distance between points B and b (along the tube) by the time lag between instants t_B and t_b.

As illustrated in Figure 5, the actual signals of the transducer may be more complex in experiments at high pressure, possibly as a result of flooding instability. Our main interest is the variation of the pressure drop along the column, $\Delta P = P_B - P_A$, with time and we have a record of $P_C - P_D$ vs. t, given by the transducer. From the diagram on the left of Figure 4, it is easily seen that $\Delta P = (P_C - P_D) + \rho_w gH$, since the tubes connecting the transducer to the column are filled with water (with density ρ_w) at all times. The constant pressure lines recorded before and after the passage of the slug correspond to the static pressure differences $\Delta P = \rho gH$ and $\Delta P = \rho_g gH$, respectively. During the process of slug rise, ΔP will vary between these two extreme values. To start with, when the nose of the slug rises between the pressure tappings, liquid will be continuously, replaced by gas in that region, and ΔP will decrease accordingly. After the nose of the slug has risen above the upper pressure tapping, and before it has reached the top of the tube, there will be upward gas flow relative to the liquid and, in the length of tube monitored by the pressure transducer, the value of ΔP can then be expressed as

$$\Delta P = \rho_g gH + \Delta P_f, \tag{5}$$

where ΔP_f accounts for the pressure drop resulting from the relative movement between gas and liquid. For high gas densities, ΔP_f may differ significantly from zero (on a scale with range ρgH, as in our measurements), as illustrated in Figure 5, where it can be seen to be an oscillating function of time.

Each plot of ΔP vs. t was manipulated to give the time average $\overline{\Delta P_f}$ and the corresponding root-mean-square fluctuation, s, in specified time intervals, and it is important to relate these time intervals with the position (relative to the nose of the slug) of the portion of the slugs scanned by the transducers. Taking the plot in Figure 5, we know that the nose of the slug is about level with the upper tapping of the transducer at time t_1 (the difference in level between the nose of the slug and the cross section for which the pressure at the tube wall becomes equal to the pressure in the slug is only a small fraction of the tube diameter). At t_2 the nose of the slug is very close to level $L_1 = u_s(t_2 - t_1)$, above the upper pressure tapping, while at t_3, its level is very nearly $L_2 = u_s(t_3 - t_1) + H$, above the lower pressure tapping. In the time interval (t_2, t_3), the pressure transducer will therefore have "scanned" the region between levels L_1 and L_2 down from

the nose of the slug, and so in our presentation of the results, we will say that the values of $grad\,(=\overline{\Delta P_f}/H)$ and $dev\,(=s/H)$ (shown on the righthand side of some plots) refer to the distance $L = L_m \pm \Delta L/2$ below the nose of the slug, where $L_m = (L_1 + L_2)/2$ and $\Delta L = L_2 - L_1$.

In each plot we use a vertical arrow to mark the instant t_C when the nose of the slug reaches the top of the tube. Fluctuations of the pressure signal are still observed for some time after t_C, because it takes a finite time for the film of liquid to run down the wall from C to the transducer, and during that time there will be a matching upward flow of gas past the transducer.

We performed experiments in the two tubes with water and mixtures of glycerol and water, covering a wide range of viscosities (see Table 1). The experiments were performed outdoors with no imposed temperature control, but care was taken to perform the experiments under approximately similar ambient conditions; after each experiment, the temperature of the liquid coming out of the tubes was measured and seen to be in the range of 16° to 23°C. (It should be noted that a series of runs with a given liquid over the whole range of pressures lasted only one half day, during which time the temperature of the test liquid remained constant to within ± 1 K.) The viscosity and density of the solutions used was determined in our laboratory over that range of temperatures, and values of the surface tension were obtained from tables of physical properties. We can see in Table 1 that to any given solution there correspond different values of the physical properties in the experiments in the two tubes. This is because the experiments with the 21-mm-ID tube were performed in winter, while those with the 32.8-mm-ID tube were performed in spring.

For each liquid, the single-slug experiment described earlier was performed at various pressures, and Figures 6 and 7 show samples of the signals obtained on the lower transducer (TR1). It is important to bear in mind that the distance, H, between the two pressure tappings leading to transducer TR1 was 0.25 m in the 21-mm-ID column (signals in Figure 6) and 0.10 m in the 32.8-mm-ID column (signals in Figure 7).

The same general trend in variation of the transducer signal with the operating pressure is observed for all the liquids. At the lower pressures the transducer signal is virtually flat, because ΔP_f is negligible; the ''waviness'' of the signal becomes increasingly apparent as the operation pressure is increased, and this trend is accompanied by a gradual increase in the value of both of $\overline{\Delta P_f}$ and s.

Figure 8 illustrates the way in which we obtained more quantitative data from the plots of ΔP vs. t. All the plots in that figure are for glycerol solution 1 in the 21 mm-ID-tube, and they are enlarged portions of the transducer signals given in Figure 6a. The signals along (i) refer to the portion of the slug at $L = 0.83 \pm 0.28$ m, down from the slug nose, those along (ii) are for $L = 1.03 \pm 0.28$ m, and those along (iii) are for $L = 1.38 \pm 0.28$ m. (The interested reader will note that $t_1 = 6$ s from Figure 6a, and $u_s = 0.15$ m/s.) Glycerol solution 1 was chosen to illustrate the results obtained, but very similar results (in general terms) were obtained with the other glycerol solutions. The results for water have been presented elsewhere (see Guedes de Carvalho et al., 2000).

Each set of three plots in a ''row'' is for a given operation pressure and the effect of this variable (that is, gas density) is clearly brought out when the signals in successive rows are compared. At the lowest pressure displayed (1.5 MPa) fluctuations in ΔP are incipient, but they gradually increase in amplitude as the operation pressure is raised; the corresponding value of *grad* and *dev*, shown on each plot, are very informative. At this point it is well to recall the observation of Dukler et al. (1984), mentioned in the Introduction, that the root-mean-square deviation of the pressure gradient undergoes a steep increase when flooding is initiated. It seems very likely that in the experiments represented in Figure 8, flooding instability set in above about 2.1 to 3.1 MPa, and although it is difficult to say with certainty the exact value of P for which the flooding instability began, it is hard not to accept that it had already happened at 3.1 MPa.

The signals from the 32.8-mm-ID tube (shown in Figure 7) were treated in a similar way to what was done in Figure 8 for the 21-mm-ID tube, and the results for both tubes are summarized in Figures 9 and 10. These figures show how the average pressure gradient and the corresponding root-mean-square fluctuation vary with operating pressure for all the experiments performed with three of the liquids, and it is obvious that only above certain values of the operating pressure does $\overline{\Delta P_f}/H$ increase markedly with P. This is strongly suggestive of a change in flow regime, and we believe it to be associated with flooding instability.

An argument against the hypothesis that flooding instability occurs in the experiments just described is that the in-

Table 1. Conditions for Inception of Flooding Instability in the Present Work

	Solution 1	Solution 2	Solution 4	Solution 6	Water
			$D = 21.0$ mm		
ρ (kg/m^3)	1,155	1,183	1,204	—	1,000
μ (Ns/m^2)	12.5×10^{-3}	32.5×10^{-3}	121.0×10^{-3}	—	1.0×10^{-3}
σ (N/m)	0.068	0.067	0.066	—	0.072
Z	115	32	5	—	3,363
P_{fl} (MPa)	2.5–3.0	2.0–2.5	1.5–2.0	—	3.0–4.0
			$D = 32.8$ mm		
ρ (kg/m^3)	1,150	1,180	1,200	1,230	1,000
μ (Ns/m^2)	11.0×10^{-3}	27.0×10^{-3}	95.0×10^{-3}	305.0×10^{-3}	1.0×10^{-3}
σ (N/m)	0.069	0.067	0.066	0.064	0.072
Z	138	41	8	2	3,363
P_{fl} (MPa)	2.0–2.5	1.5–2.0	1.0–1.5	0.6–1.0	2.5–3.0

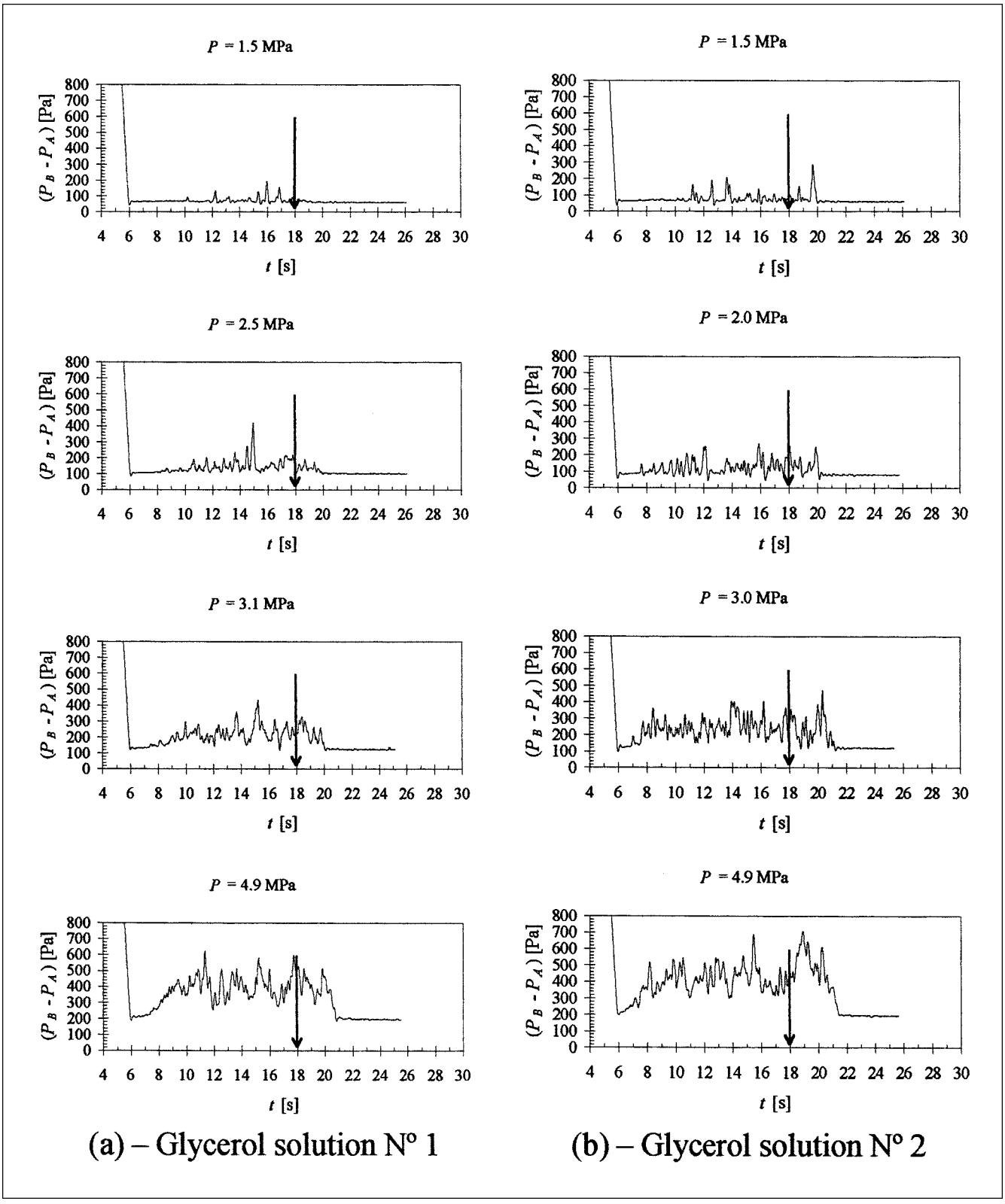

Figure 6. Signals from lower-pressure transducer in 21-mm ID-tube *(continued).*

$H_1 = 0.25$ m; the vertical arrow marks the instant t_C, when the slug reaches the top of the tube.

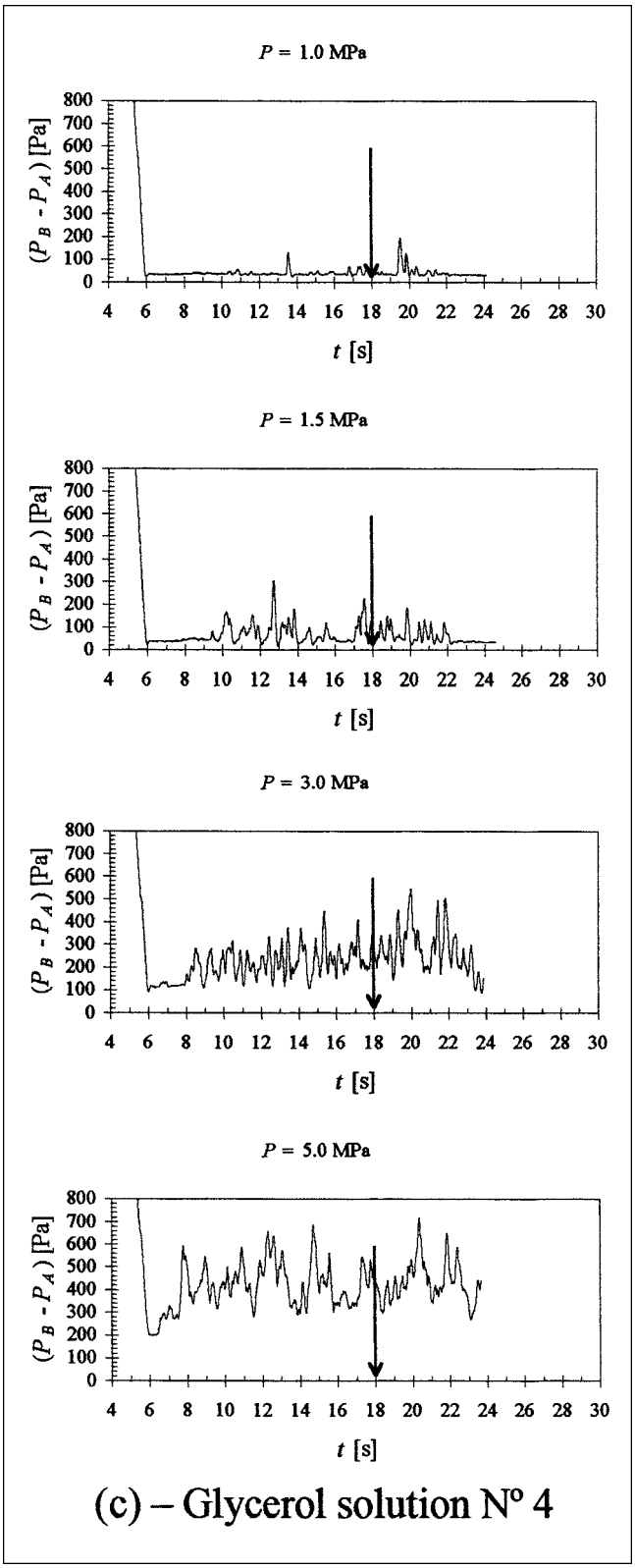

Figure 6. *(Continued)* Signals from lower-pressure transducer in 21-mm ID-tube.

$H_1 = 0.25$ m; the vertical arrow marks the instant t_C, when the slug reaches the top of the tube.

crease in $\overline{\Delta P_f}$ with P is not as steep as is usually reported for the corresponding variation of $\overline{\Delta P_f}$ with U in wetted wall tubes. With regard to this point, it is important to bear in mind that the value of $\rho_g u_r^2$ is more strongly dependent on gas velocity than on gas density, and it is the value of $\rho_g u_r^2$ that is likely to determine the inception of flooding instability. Also, in classic experiments on flooding, the pressure drop is often measured across the whole length of the test tube, even though the wetted-wall flow takes place over only the lower portion of that tube. When flooding sets in, liquid is thrown up against the wall of the upper portion of the tube (previously dry), with a consequent substantial increase in pressure drop in the gas, as is well illustrated by the work of Dukler et al. (1984).

Strong support for our view (that flooding instability occurred at the higher pressures in the experiments with slugs) also comes from an inspection of the magnitude of the average pressure gradient. Figure 10 shows that the value of $\overline{\Delta P_f}/H$ in the 32.8-mm tube were as high as 800 N/m^3 with water (and higher with the glycerol solutions) at the higher operating pressures, while Hewitt et al. (1965), who worked with water in a 32-mm tube, report that flooding was initiated whenever the pressure gradient exceeded about 90 N/m^3. In view of the direct proportionality between interfacial shear stress and pressure gradient (see Eq. 4), it is difficult to accept that this near tenfold increase in shear stress is not accompanied by flooding instability.

In comparing our work with traditional experiments on flooding in wetted-wall columns, it might be argued that in our experiments, W will be equal to zero, since no liquid can be carried up across the nose of the slug. This is obviously true in the vicinity of the nose of the slug, where the relative velocity between gas and liquid falls to zero (accordingly, there is no fluctuation in ΔP near the left corner of the ''valley'' of the transducer signals in Figures 6 and 7, although this may be partly due to the decreased amplitude of interfacial waves). Further down the slug, however, where the velocity profiles for gas and liquid are similar to those in a wetted-wall column, liquid may be ripped from the falling film and dragged into the tube core. This liquid will be returned to the falling film at some higher level on a reference frame moving with the film, even though it will probably be at a lower level on a frame attached to the tube wall. Some authors consider flooding to be characterized by the upward flow of liquid, relative to the tube wall, and that is why we prefer to talk of flooding instability when fluctuations in ΔP start to show vividly, as in our experiments at the higher operating pressures.

We summarize our observations in Table 1, where P_{fl} represents the pressure interval within which we think that flooding instability was initiated for the different liquids in each of the two tubes.

An attempt at correlating the data obtained in our experiments with those on flooding in wetted-wall columns, operating with air at atmospheric pressure, is presented in the following section.

Theory

The detailed mechanics of flooding is a complex problem, and the theories developed so far to explain it have not led to

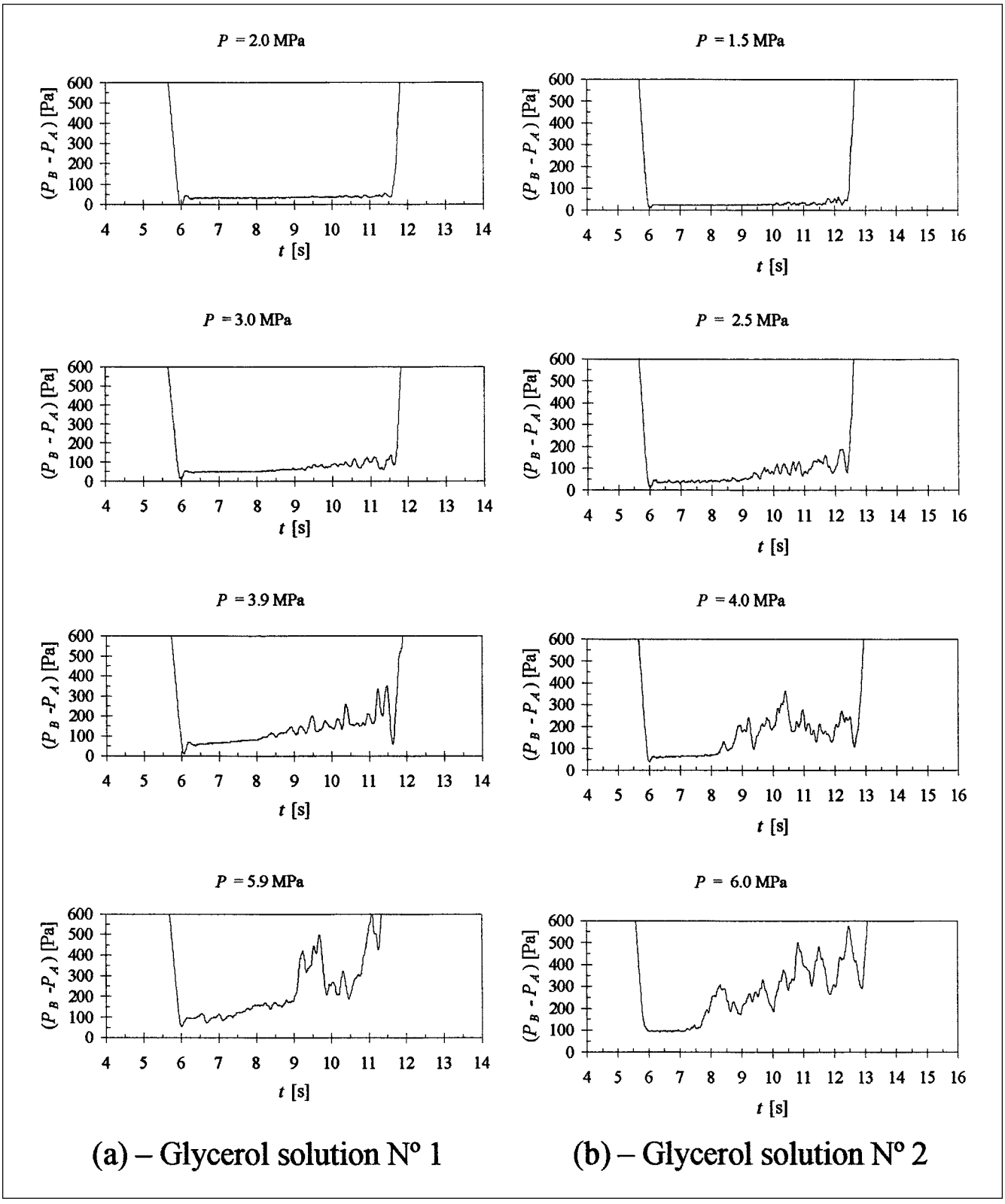

Figure 7. Signals from lower-pressure transducer in 32.8-mm-ID tube *(continued).*

$H_1 = 0.10$ m; in these experiments the slug reached the top of the tube after the bottom of the slug reached the pressure tappings.

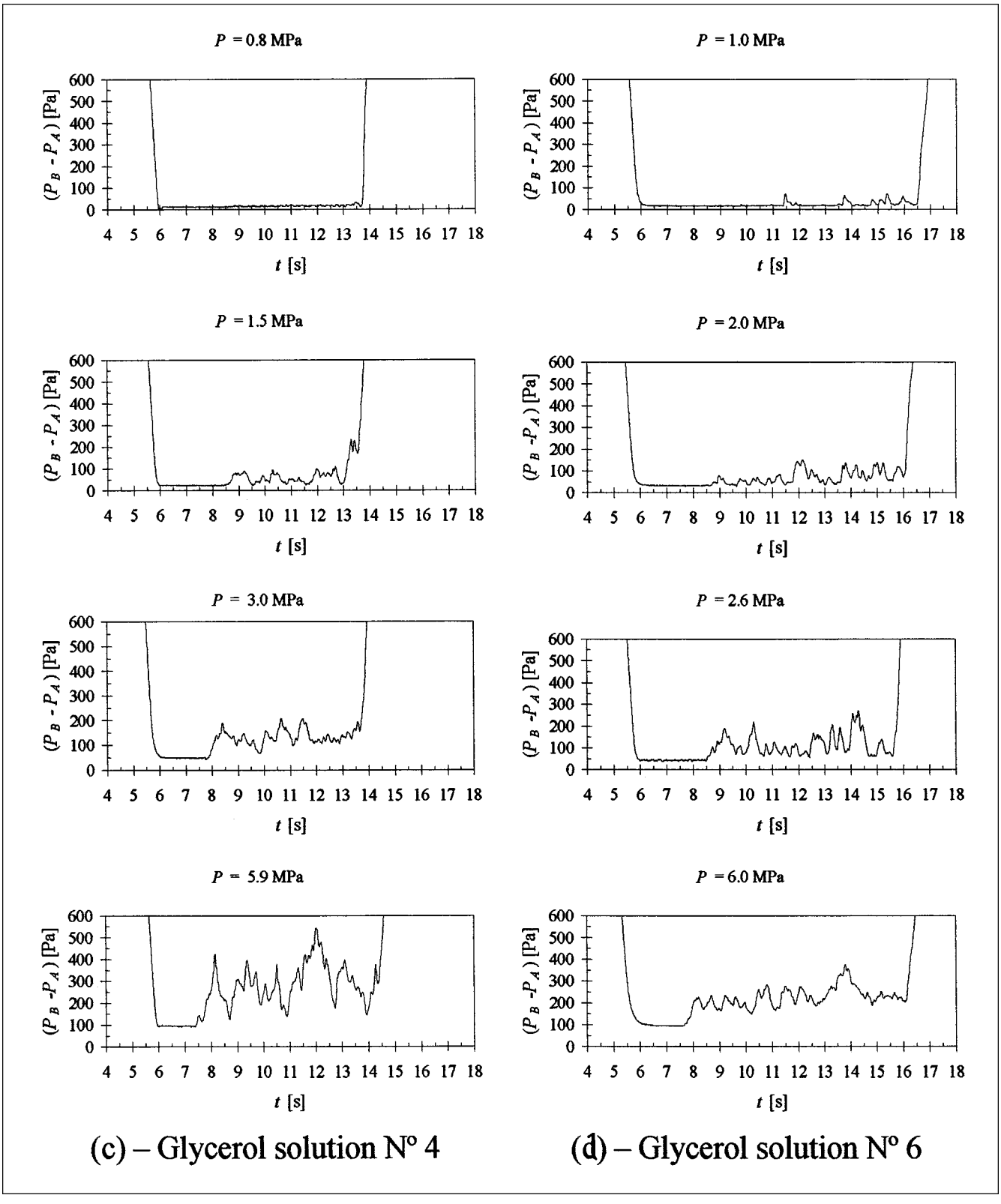

Figure 7. *(Continued)* Signals from lower-pressure transducer in 32.8-mm-ID tube.

$H_1 = 0.10$ m; in these experiments the slug reached the top of the tube after the bottom of the slug reached the pressure tappings.

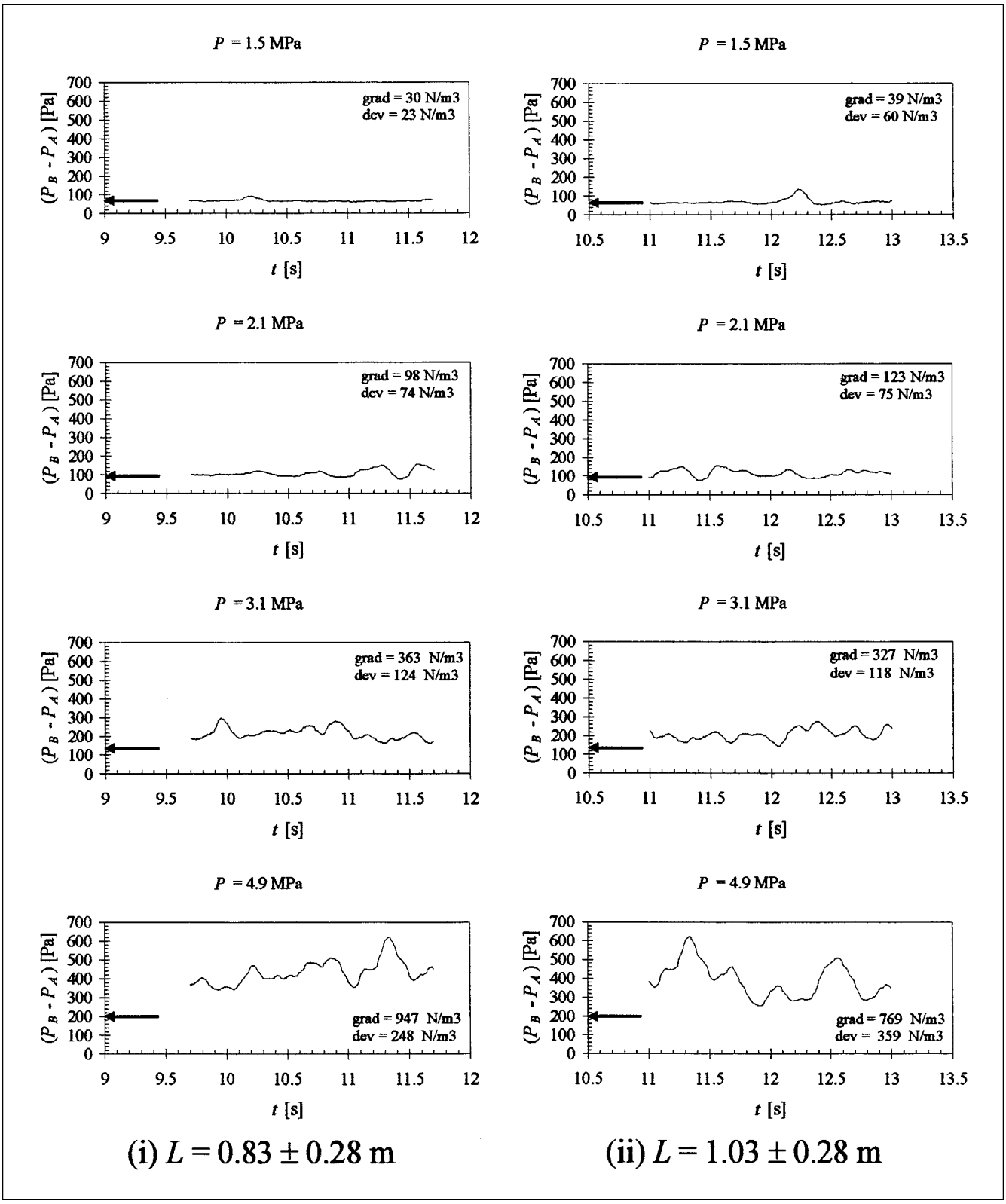

Figure 8. Selected intervals of transducer signals for slugs in 21-mm-ID tube with glycerol solution 1.

The signals shown are enlarged portions of those in Figure 6a, and the arrow indicates the static-pressure difference.

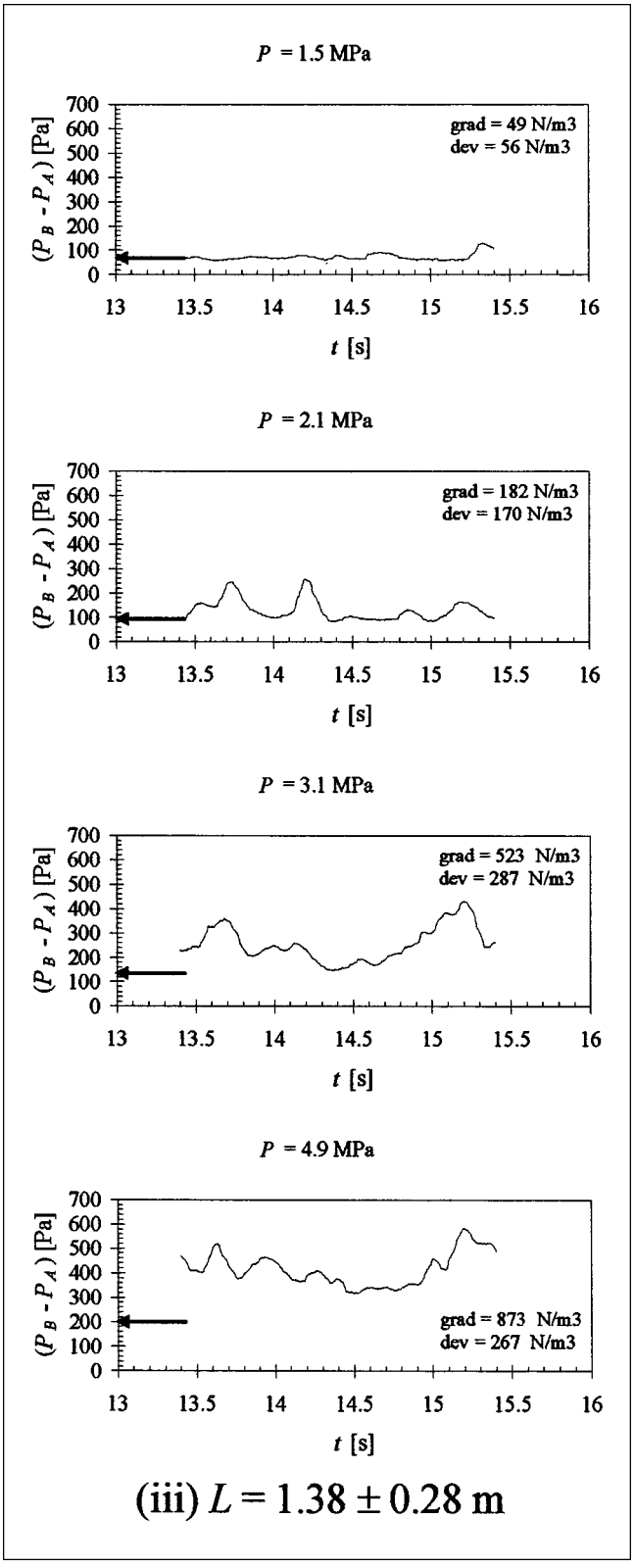

Figure 8. *(Continued)* Selected intervals of transducer signals for slugs in 21-mm-ID tube with glycerol solution 1.

The signals shown are enlarged portions of those in Figure 6a, and the arrow indicates the static-pressure difference.

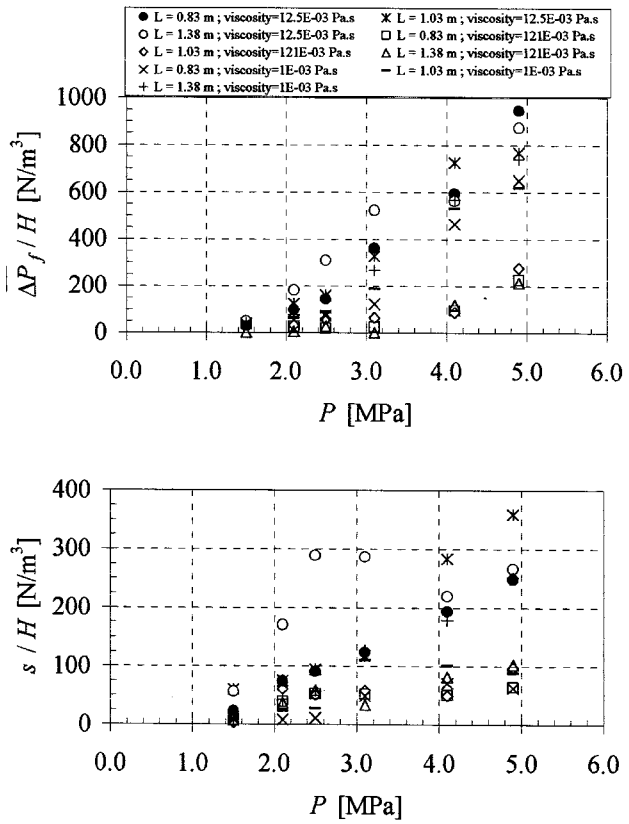

Figure 9. Average pressure gradients along individual slugs and corresponding root-mean-square fluctuations for 21-mm-ID tube.

satisfactory quantitative criteria. For that reason, experimental studies abound, and the large number of data collected have been used to formulate a variety of empirical correlations. Extensive reviews of the topic, for example, by McQuillan and Whalley (1985) and Bankoff and Lee (1986), are available.

In the present article we make no attempt at deriving a detailed analytical description of flooding, but use physical insight to help establish the laws relating the dominant variables.

To start with, it is important to refer again to Figure 2, where a classic arrangement for experiments on countercurrent annular flow is sketched. Two important parameters to be considered in our analysis are the thickness (δ) of the film of liquid running along the wall and the velocity (u_i) on the interface. In the absence of gas movement, the corresponding expressions for laminar flow are (see Wallis, 1969)

$$\delta = 0.909\left(\frac{\nu^2}{g\gamma}\right)^{1/3} Re^{1/3} \tag{6}$$

and

$$u_i = 0.413(g\nu\gamma)^{1/3} Re^{2/3}, \tag{7}$$

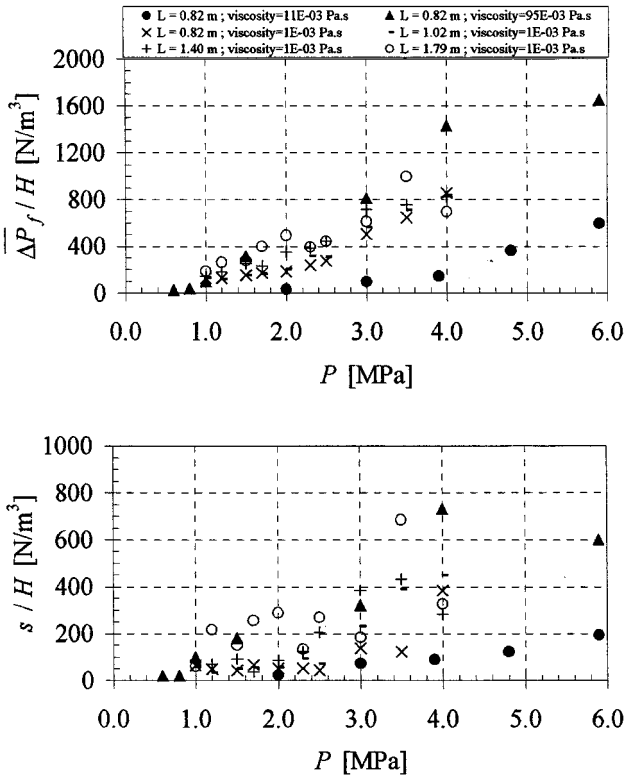

Figure 10. Average pressure gradients along individual slugs and corresponding root-mean-square fluctuations for 32.8-mm-ID tube.

whereas for turbulent flow they are

$$\delta = 0.135\left(\frac{\nu^2}{g\gamma}\right)^{1/3} Re^{7/12} \tag{8}$$

and

$$u_i = 1.85a(g\nu\gamma)^{1/3} Re^{5/12}, \tag{9}$$

where $\alpha = u_i\delta/Q$ is the ratio between the velocity of the liquid on the interface and the average velocity of the liquid in the film. Equation 8 follows directly from the work of Belkin et al. (1959), while Eq. 9 is a simple extension of the analysis of Dukler and Bergelin (1952). The value of α varies from 1.36, for $Re = 2{,}056$, to an asymptotic 1.15, for large Re, but taking $a = 1.2$ will often be a good approximation for the entire turbulent range. The transition between laminar and turbulent film flow is expected to occur somewhere in the range $1{,}000 < Re < 4{,}000$ [such as Fulford, 1964; or Aragaki et al., 1990].

In countercurrent flow, there will be an upward shear stress exerted by the gas on the liquid, but it can be shown (see Guedes de Carvalho and Talaia, 1998) that, up to the flooding point, its magnitude will correspond to only a small fraction of the weight of liquid per unit interfacial area; as a result, Eqs. 6 to 9 will still be very nearly correct, up to the flooding limit.

However, it is well to remember that the idea of a smooth film of constant thickness, δ, is an approximation. Indeed, the use of advanced photographic techniques revealed the existence of small-amplitude waves on the surface of falling liquid films (such as Belkin et al., 1959; Hewitt and Wallis, 1963), and the characteristics of such waves have been followed by means of conductance probes (see Hewitt and Wallis, 1963; Zabaras and Dukler, 1988; Biage et al., 1989). The latter group studied flooding in flow along a flat wall in a ''rectangular'' channel.

The results of all these studies are in general agreement and, as expected from theoretical predictions, it was found that waves grow in amplitude as they move down the wall and that an up-flowing gas stream enhances that tendency. This increase in wave amplitude with distance to the liquid feed explains why flooding velocities decrease with an increase in the length of the test section (other things being equal), as discovered by Hewitt et al. (1965), among others.

Curiously, for gas velocities up to the flooding point, the average values of wave velocity, measured by Zabaras and Dukler (1988) and by Biage et al. (1989), are in close agreement with interfacial liquid velocities given by Eq. 7 or Eq. 9; it is only for gas velocities above the flooding limit that a decrease in the velocity of the waves is observed. This finding is of particular relevance to the physical reasoning presented below.

Although the general succession of events that lead to flooding in countercurrent annular film flow is well known, it should be pointed out that there is still much doubt about the detailed mechanism of the process. One possible view is that flooding will occur when the force exerted by the gas on the individual waves traveling down the interface is such that it leads to an ''exponential'' growth of the wave, followed by a ''back splash'' of the liquid. This mechanism is very much like that suggested initially by Shearer and Davidson (1965), and it has recently been the object of computer simulations by Jayanti et al. (1996). An alternative view is that the force exerted by the gas on the liquid gradually leads to a ''wrinkling'' of the interface and that the wrinkled interface ''yields'' (possibly also with the formation of large waves) when the interfacial shear stress is increased above some threshold value. The observations of Biage et al. (1989) seem to support this view and the idea has been explored further by Guedes de Carvalho and Talaia (1998) for films of water and Guedes de Carvalho et al. (1999) for films of viscous liquids.

Here we follow the view that flooding is the outcome of waves growing very fast in response to the drag exerted by the gas.

In Figure 11 the waves are sketched as equal sized and moving down with velocity u_w (positive downward), with the gas moving up with velocity u (positive upward). The relative velocity between gas and waves is given by $u_r = u_w + u$, and it is important to consider the relative magnitudes of u and u_w. Zabaras and Dukler (1988) and Biage et al. (1989) found that, up to the flooding point, u_w is very close to u_i (given by Eq. 7 or Eq. 9), and therefore $u_r \cong u + u_i$. The majority of the experiments on flooding reported in the literature (see McQuillan and Whalley, 1985) were performed at atmospheric pressure, with $Re < 5000$, and this resulted in values of u_i of the order of 1 m/s, and values of u typically in the range 4–10 m/s. Taking $u_r \cong u$ instead of $u_r \cong u + u_i$ did not introduce a

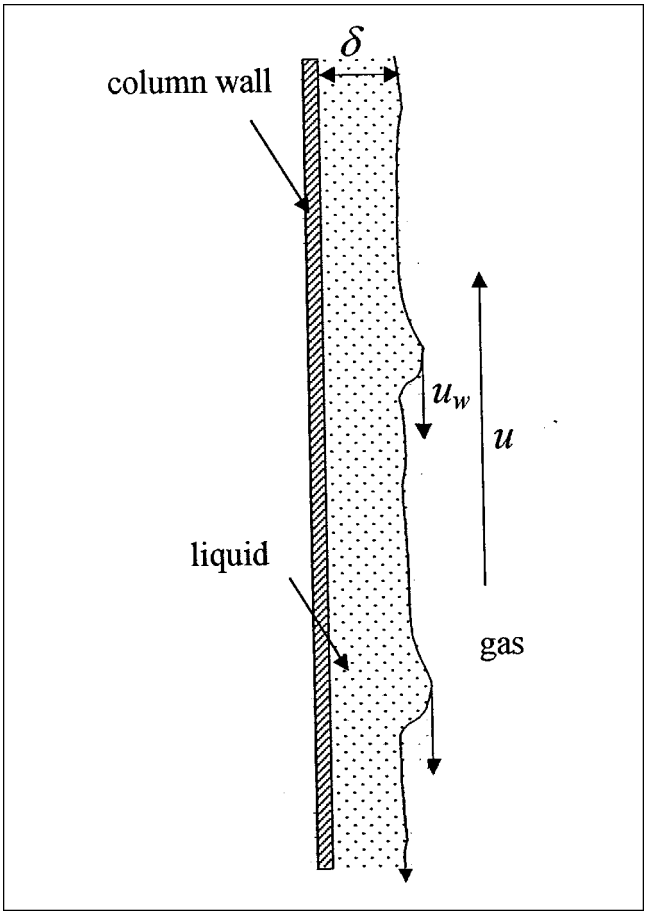

Figure 11. Film flow with waves ($u_w \approx u_i$).

significant error. With high gas densities, however, values of u are expected to be much lower, and u_i will be a significant fraction of u_r.

The rate of growth of the interfacial waves is largely determined by the drag exerted on them by the gas (see Shearer and Davidson, 1965), and therefore $\rho_g u_r^2$ will be an important parameter in determining the occurrence of flooding instability. If a series of experiments, as in Figure 2, is carried out in a given tube at a fixed flow rate of a given liquid, over a range of gas densities, it may be expected that flooding instability will always be initiated at the same value of $\rho_g u_r^2$, which we denote by $(\rho_g u_r^2)_{fl}$.

For a different liquid or for a different flow rate of the same liquid, the value of $(\rho_g u_r^2)_{fl}$ may be expected to be different and it is reasonable to write

$$\left(\rho_g u_r^2\right)_{fl} = \phi(\rho, \mu, \sigma, g, Q), \tag{10}$$

where σ is the surface tension of the liquid. Dimensional analysis will then lead to

$$\frac{\left(\rho_g u_r^2\right)_{fl}}{(\rho g \sigma)^{1/2}} = f(Re, Z), \tag{11}$$

where $Re = 4Q/\nu$ and $Z = \sigma(\rho/g\mu^4)^{1/3}$, and this result is seen to be similar to that obtained by Shearer and Davidson (1965), with the important difference that u_r, instead of u, is now used in the dimensionless group expressing the force exerted by the gas on the waves.

Two restrictions on the presumed validity of Eq. 11 are worth mentioning. First, the amplitude of the waves moving along the interface is known to increase with distance below the liquid feed; in that respect, Eq. 11 is strictly only applicable for the constant distance below the feed point. Second, the curvature of the vertical surface along which the liquid flows is not being taken into account, and this means that for flow along the wall of small-diameter tubes, an additional dimensionless group will be required on the righthand side of Eq. 11. If these two restrictions are ignored, as a first approximation data on flooding for a given liquid (that is, for constant Z) should fall on a single line in a plot of M vs. Re, where $M = (\rho_g u_r^2)_{fl}/(\rho g \sigma)^{1/2}$. Some scatter is to be expected, because the velocity of flooding is somewhat dependent on the height of the column used in the experiments and on the methods of feeding liquid and gas.

Comparison of Theory With Experiment

Most experiments on flooding in wetted-wall tubes reported in the literature are for water and air at atmospheric pressure, but a few data are available for more viscous liquids, also with air at atmospheric pressure. In Figures 12 and 13 we plot the relevant data in appropriate form (after calculating u_r from reported values of flooding velocity and liquid flow rate) together with those obtained from our experiments with single slugs.

With regard to our own data, it should be remembered that only one value of Re is obtained with any given liquid in a given column, because of the fact that u_s is then uniquely determined (apart from minor variations in $\gamma^{1/2}$). Furthermore, the relative uncertainty about the exact value of P at which flooding instability can be considered to start, will show as an uncertainty in M; in the plots, we use two points connected by a line segment to specify the range of values of M over which flooding instability is thought to have been initiated.

Three plots were organized in Figure 12 to cover different ranges of Z (and accordingly of Re) without loss of readability on linear scales. The points cover a wide range of experimental conditions, including different tube diameters and tube lengths. The data of Clift et al. (1996) and our own for the 32.8-mm-ID tube are in alignment and so are the points of Suzuki and Ueda (1977) and our own for the 21-mm-ID tube. In Figure 12b, the values obtained from Tobilevich et al. (1968) are much too low, but this is probably due to the technique used by those authors, as pointed out by Guedes de Carvalho and Talaia (1998). In Figure 12c, the values from Clift et al. (1966) are high in comparison with those of Celata et al. (1992), and this is probably showing the effect of the diameter (already in Figures 12a and 12b, the data of Clift et al. (1966) are higher than "expected" in comparison with those of Suzuki and Ueda (1997)).

It is worth emphasizing the agreement between our own data and those obtained in wetted-wall columns for similar values of Z; particularly since the value of $u_r (= u_i + u)$ is largely determined by u_i in our experiments, and by u in the

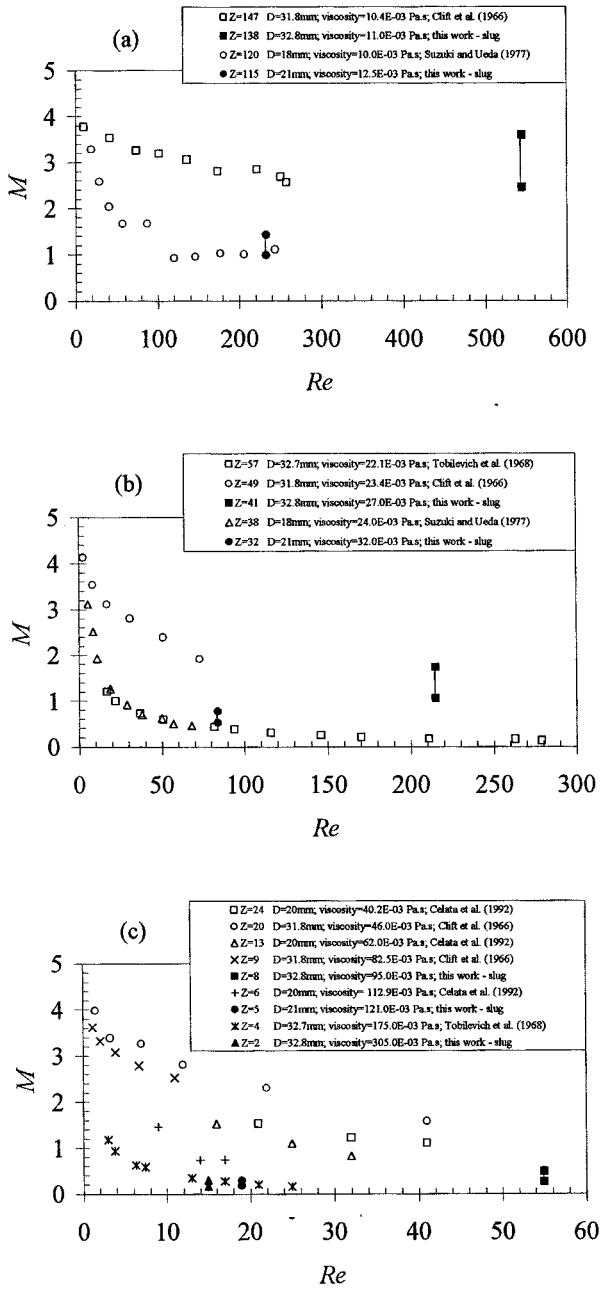

Figure 12. *M* vs. *Re* for viscous liquids over three ranges of *Z*.

experiments reported by other authors. The reader's attention is also drawn to the fact that M is proportional to u_r^2; consequently, relative uncertainties in u_r are doubled in M.

The results displayed in Figure 12 for viscous liquids seem to give strong theoretical support to the idea that flooding is likely to have occurred at the operating pressures suggested by our experiments.

For the air–water system, Guedes de Carvalho and Talaia (1998) reviewed critically a significant number of studies on flooding, and selected four series of data from different authors who worked with similar-size tubes to illustrate the wide scatter in the flooding velocities reported. Such scatter in the raw data will be amplified in the plot of M vs. Re, but critical

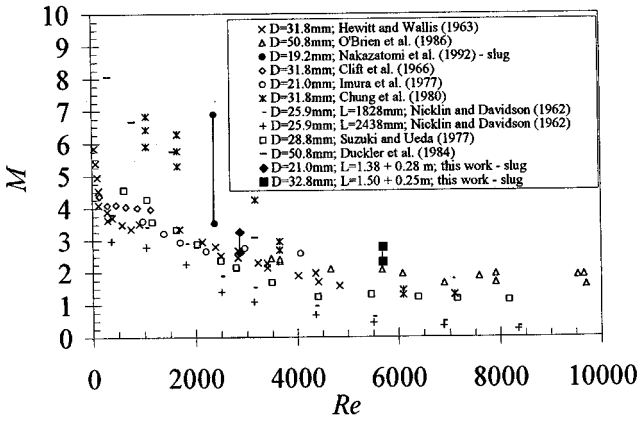

Figure 13. *M* vs. *Re* for water.

assessment of the data reviewed led to a smaller collection of experimental points as possibly representative of the air–water system in tubes with $D > 20$ mm. Those points are plotted in Figure 13, together with data from our work and that of Nakazatomi et al. (1992), who studied the rise of long nitrogen slugs in a 19.2-mm-ID vertical tube filled with water at pressures up to 20 MPa. The experiments of Nakazatomi et al. (1992) were performed at discrete values of the operating pressure (0.3, 5, 10, 15 and 20 MPa), and the occurrence of "ephemeral large waves" was detected only when the operation pressure was raised above 5 MPa. From the detailed account given by the authors, it is clear that the formation of these ephemeral large waves is a clear sign of flooding instability. The range in values of M corresponding to the 5- to 10-MPa interval is represented by a line segment in Figure 13. The points from the present work are also plotted with a vertical line segment superposed to show the range of values of M over which flooding instability is thought to have been initiated.

The general alignment of the points in Figure 13 is not remarkable, but if it is considered that flooding velocities are strongly dependent on the length of the test section and that M is proportional to the square of the relative velocity between gas and liquid, the lack of alignment can be seen as scatter. It is worth mentioning that a similar alignment of the data points is obtained when the phenomenon of flooding is interpreted as the result of an interfacial shear stress "threshold" being reached, as was done by Guedes de Carvalho and Talaia (1998). The latter interpretation leads to the conclusion that the value of $\rho_g^{3/4} u_r^{7/4}$, rather than $\rho_g u_r^2$, determines the occurrence of flooding instability. The difference between the predictions of the two criteria is shown in Figure 14 and more accurate data will be needed to discriminate between them.

Empirical correlations

In the absence of any accurate theory, the occurrence of flooding is normally predicted by means of empirical correlations. From the review of McQuillan and Whalley (1985), two correlations stand out. The correlation of Wallis (1961) has widespread popularity, partly as a result of its simple form:

$$\sqrt{U_l^*} + \sqrt{U_g^*} = C, \tag{12}$$

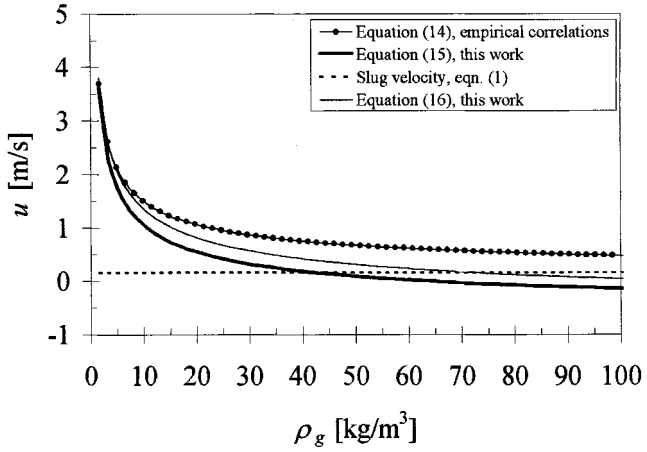

Figure 14. Dependence of flooding velocity on gas density (for glycerol solution 1 in 21-mm tube at *Re* = 235).

where

$$U_l^* = U_l\left[\frac{\rho}{gD(\rho-\rho_g)}\right]^{1/2} \quad \text{and}$$

$$U_g^* = U_g\left[\frac{\rho_g}{gD(\rho-\rho_g)}\right]^{1/2}.$$

Here U_l and U_g are the superficial velocities of liquid and gas, respectively, and C is a constant, typically with a value between 0.8 and 1.0.

The correlation of Alekseev et al. (1972), modified by McQuillan and Whalley (1985), is claimed by these authors to give best overall accuracy, and it can be expressed as

$$K_g = 0.286\,Bo^{0.26}Fr^{-0.22}\left(1+\frac{\mu}{\mu_w}\right)^{-0.18}, \qquad (13)$$

where

$$K_g = \left(U_g\rho_g^{1/2}\right)/\left[g\sigma(\rho-\rho_g)\right]^{1/4}$$

$$Bo = D^2 g(\rho-\rho_g)/\sigma$$

$$Fr = Q\left[g(\rho-\rho_g)^3/\sigma^3\right]^{1/4}$$

and μ/μ_w is the ratio between the viscosity of the liquid under study and that of water at 20°C.

The reader will have no difficulty confirming that neither of these correlations predicts the occurrence of flooding in our experiments with isolated slugs in the range of pressures studied, and it is important to understand why they fail to do so.

If we consider the rise of a single slug in a given tube filled with a given liquid, and if we imagine the experiment performed over a range of pressures, the value of u_s will be very nearly constant and independent of the operating pressure. As a result, the values of U_l, U_g, and Q will be nearly independent of pressure, and even the value of $\rho-\rho_g$ will vary only slightly for pressures in the range 0.1 to 6 MPa (with argon or nitrogen). A close inspection of Eqs. 12 and 13 shows that, under these constraints, they both predict the occurrence of flooding at a constant value of $\rho_g^{1/2}U_g$ (or equivalently of $\rho_g U_g^2$). This is at variance with our suggestion, explained earlier, that the occurrence of flooding (for a single slug rising in a given liquid in a given tube) is expected to be observed for constant $\rho_g u_r^2$.

In order to better illustrate these different predictions, we consider the case of a mixture of glycerol and water with the properties of our solution No. 1 (see Table 1) in the 21-mm-ID tube ($Z = 115$). In the single-slug experiment in the 21-mm-ID tube, $u_s = 0.156$ m/s (from Eq. 1) in the pressure range of interest (say, up to 4 MPa), and this will result in $Re = 235$ for the film of liquid around the slug (from Eqs. 3 and 6).

We start by estimating the velocity of flooding that would be observed with air at atmospheric pressure in a wetted-wall tube of 21 mm ID, operating with the same liquid, also at $Re = 235$. Both Eq. 12, with $C = 1$, and Eq. 13, predict $U_g = 3.3$ m/s, and this is also the value obtained by Suzuki and Ueda (1977) in their experiments in a 18-mm-ID tube with a glycerol solution for which $Z = 120$ at $Re = 244$ (which is near enough to the conditions that we are examining).

From Eqs. 6 and 7, we obtain the values $\delta = 1.3$ mm and $u_i = 0.74$ m/s (for $Re = 235$ with our glycerol solution 1), and therefore $u = U_g D^2/(D-2\delta)^2 = 4.3$ m/s and $u_r = u + u_i = 5.0$ m/s, with air at atmospheric pressure ($\rho_g = 1.21$ kg/m^3).

The predicted law of variation of u with gas density (at constant Re for the liquid) is then $u^2\rho_g = 4.3^2 \times 1.21$ kg·m^{-1}·s^{-2} from both the correlation of Wallis (1961), and that of Alekseev et al. (1972), modified by McQuillan and Whalley (1985), and this can be expressed as

$$u = 4.73\rho_g^{-1/2}, \qquad (14)$$

with u and ρ_g in SI units.

From the interpretation of flooding developed in the present work, the dependence of u on gas density for the situation under consideration (also at constant Re for the liquid) would be $(u+0.74)^2\rho_g = (4.3+0.74)^2 \times 1.21$ kg·m^{-1}·s^{-2}, and this can be expressed as

$$u = 5.54\rho_g^{-1/2} - 0.74, \qquad (15)$$

where u and ρ_g are again in SI units.

The assumption that the value of $\rho_g^{3/4}u_r^{7/4}$ determines the inception of flooding instability, which follows from the work of Guedes de Carvalho and Talaia (1998), can be shown to lead to

$$u = 5.62\,\rho_g^{-3/7} - 0.74 \qquad (16)$$

in the situation under study (u and ρ_g are again in SI units).

In Figure 14 we plot the predicted dependence of u on ρ_g given by Eqs. 14, 15, and 16, and we also show (by a dotted

line) the value of the rise velocity of the slugs in the 21-mm-ID tube, given by Eq. 1. In the single-slug experiments, flooding instability is predicted to be observed at those gas densities for which $u < u_s$. According to Eq. 15 this will happen for $\rho_g > 42$ kg/m^3, which is the density of argon at $P > 2.4$ MPa. From Eq. 16 the instability is predicted to start at $\rho_g \cong 73$ kg/m^3, which is the density of argon at $P \cong 4.4$ MPa. From Table 1 it can be seen that 2.5 MPa $< P_{fl} <$ 3.0 MPa for the slugs of argon in solution 1 in the 21-mm tube, and this is in very good agreement with the prediction in Eq. 15.

Equation 14 does not predict the occurrence of flooding in the single-slug experiments at gas densities up to 300 kg/m^3.

A further point to be noted in Figure 14 is the prediction of flooding instability with negative u, at gas densities above about 60 kg/m^3. Although this may be surprising at first, it follows from the fact that with negative u, but with $|u| < u_i$, there is still an upward movement of gas relative to the liquid. The waves on the interface still will be subject to the drag exerted by the gas, and for sufficient gas density, this will presumably lead to fast growth in wave amplitude, accompanied by a significant decrease in wave velocity (Nakazatomi et al., 1992 detected this type of behavior in film flow around high-density gas slugs rising in water). Tearing of these fast growing waves will follow, as reported by Suzuki and Ueda (1977) and Jayanti et al. (1993), among others, for work at atmospheric pressure, and the drops formed will be carried up in the gas stream. At high pressure, however, flooding instability is expected to start with very low or negative gas velocities, and any drops formed by tearing of the wave crests still will be moving up relative to the liquid film, even though they may be moving down relative to the tube wall. It may be worth stressing here that the present work is only concerned with the inception of flooding instability.

Concluding Remarks

Continuous measurements of pressure gradient were made along single slugs of argon rising in vertical tubes filled with liquid, with viscosities in the range 10^{-3} to 305×10^{-3} Pa·s, over a range of absolute pressures up to 6 MPa.

With all the liquids tested, it was observed that the average value of the pressure gradient (and its root-mean-square fluctuations) along the slugs rose steeply with the operation pressure (that is, gas density) when this variable was increased above about 1.5 to 2.5 MPa, the exact value depending on the liquid and on the diameter of the vertical tube.

Since the flow pattern of gas and liquid at a significant distance down from the nose of the slugs is the same as in a wetted-wall column, the results from our work are of direct relevance to the understanding of the operation of this type of equipment. And with average values of the pressure gradient of up to about 900 N/m^3 both in the 21-mm-ID and in the 32.8-mm-ID tubes, we are led to conclude that flooding instability must have occurred in the film flowing around the slugs for the higher gas densities.

A simple physical interpretation of the phenomenon of flooding in wetted-wall columns is also presented, and dimensional analysis is used to show that our data, obtained at high operating pressures, are in close agreement with those on flooding, obtained by other authors in wetted-wall tubes operating at atmospheric pressure.

Additionally, our work reveals major weaknesses in the empirical correlations currently used in the prediction of flooding in film flow in wetted-wall tubes.

Notation

Bo = dimensionless group defined below Eq. 13
Fr = dimensionless group defined below Eq. 13
K_g = dimensionless group defined below Eq. 13
ΔL = length of portion of slug scanned by transducer
ΔP_f = irreversible pressure drop between points B and A, N·m^{-2}
U_g^* = dimensionless gas velocity defined below Eq. 12
U_l^* = dimensionless liquid velocity defined below Eq. 12
Z = liquid property group $[= \sigma(\rho/g\mu^4)^{1/3}]$
μ = dynamic viscosity of liquid, Pa·s

Literature Cited

Alekseev, V. P., A. E. Poberezkin, and P. V. Gerasimov, "Determination of Flooding Rates in Regular Packings," *Heat Transfer Sov. Res.*, **4**, 159 (1972).

Aragaki, T., S. Toyama, H. M. Salah, K. Murase, and M. Suzuki, "Transitional Zone in a Falling Liquid Film," *Int. Chem. Eng.*, **30**, 495 (1990).

Bankoff, S. G., and S. C. Lee, "A Critical Review of the Flooding Literature," *Multiphase Science and Technology*, Vol. 2, G. F. Hewitt, J. M. Delhaye and N. Zuber, eds., Hemisphere, Washington (1986).

Belkin, H. H., A. A. MacLeod, C. C. Monrad, and R. R. Rothfus, "Turbulent Flow Down Vertical Walls," *AIChE J.*, **2**, 245 (1959).

Biage, M., J. M. Delhaye, and Ph. Vernier, "The Flooding Transition: A Detailed Experimental Investigation of the Liquid Film Flow Before the Flooding Point," *ANS Proc. National Heat Transfer Conf.*, ANS, p. 53 (1989).

Celata, G. P., M. Cumo, T. Setaro, and S. Banerjee, "A Model for Flooding Prediction in Circular Tubes," *J. Therm. Sci.*, **1**, 166 (1992).

Clift, R., C. L. Pritchard, and R. M. Nedderman, "The Effect of Viscosity on the Flooding Conditions in Wetted Wall Columns," *Chem. Eng. Sci.*, **21**, 87 (1966).

Dukler, A. E., and O. P. Bergelin, "Characteristics of Flow in Falling Liquid Films," *Chem. Eng. Prog.*, **48**, 557 (1952).

Dukler, A. E., L. Smith, and A. Chopra, "Flooding and Upward Film Flow in Tubes—Experimental Studies," *Int. J. Multiphase Flow*, **10**, 585 (1984).

Fulford, G. D., "The Flow of Liquids in Thin Films," *Adv. Chem. Eng.*, **5**, 151 (1964).

Guedes de Carvalho, J. R. F., and M. A. R. Talaia, "Interfacial Shear Stress as a Criterion for Flooding in Counter Current Film Flow Along Vertical Surfaces," *Chem. Eng. Sci.*, **53**, 2041 (1998).

Guedes de Carvalho, J. R. F., M. A. R. Talaia, and M. J. F. Ferreira, "Flooding of High Density Gas Slugs Rising in Viscous Liquids," *Proc. Int. Symp. on Two-Phase Flow Modelling and Experimentation*, Pisa, Italy, 771 (1999a).

Guedes de Carvalho, J. R. F., M. A. R. Talaia, and M. J. F. Ferreira, "Flooding Instability of High Density Gas Slugs Rising in Vertical Tubes Filled with Water," *Chem. Eng. Sci.* (in press, 2000).

Hewitt, G. F., and G. B. Wallis, "Flooding and Associated Phenomena in Falling Film Flow in a Vertical Tube," *Proc. Multiphase Flow Symp.—Winter Annual Meeting of ASME*, Philadelphia, p. 62 (1963).

Hewitt, G. F., P. M. C. Lacey, and B. Nicholls, "Transition in Film Flow in a Vertical Tube," AERE-R4614, UKAEA, Harwell, England (1965).

Jayanti, S., A. Tokarz, and G. F. Hewitt, "Theoretical Investigation of the Diameter Effect on Flooding in Countercurrent Flow," *Int. J. Multiphase Flow*, **22**, 307 (1996).

McQuillan, K. W., and P. B. Whalley, "A Comparison Between Flooding Correlations and Experimental Flooding Data for Gas-Liquid Flow in Vertical Circular Tubes," *Chem. Eng. Sci.*, **40**, 1425 (1985).

Nakazatomi, M., H. Shimizu, G. Miyake, and K. Sekoguchi, "Rising Characteristics of a Single Measure of Gas Slug in Stagnant Liquid —Effect of Pressure," *JSME Int. J.*, Series II, **35**, 388 (1992).

Nicklin, D. J., and J. F. Davidson, ''The Onset of Instability in Two-Phase Slug Flow,'' *Proc. Inst. Mech. Eng. Symp. Two-Phase Flow*, London, p. 29 (1962).
Nicklin, D. J., J. O. Wilkes, and J. F. Davidson, ''Two-Phase Flow in Vertical Tubes,'' *Trans. Inst. Chem. Eng.*, **40**, 61 (1962).
Shearer, C. J., and J. F. Davidson, ''The Investigation of a Standing Wave Due to Gas Blowing Upwards over a Liquid Film; Its Relation to Flooding in Wetted-Wall Columns,'' *J. Fluid Mech.*, **22**, 321 (1965).
Suzuki, S., and T. Ueda, ''Behaviour of Liquid Films and Flooding in Counter Current Two Phase Flow—1. Flow in Circular Tubes,'' *Int. J. Multiphase Flow*, **3**, 517 (1977).
Tobilevich, N. Y., I. I. Sagan, and Y. G. Porzhezihskii, ''The Downward Motion of a Liquid Film in Vertical Tubes in an Air-Vapour Counterflow,'' *J. Eng. Phys.*, **15**, 855 (1968).
Wallis, G. B., ''Flooding Velocities for Air and Water in Vertical Tubes,'' UKAEA, Rep. AEEW-R123, Harwell, England (1961).
Wallis, G. B., *One-Dimensional Two-Phase Flow*, McGraw-Hill, New York (1969).
Zabaras, G. J., and A. E. Dukler, ''Countercurrent Gas-Liquid Annular Flow, Including the Flooding State,'' *AIChE J.*, **34**, 389 (1988).

Manuscript received June 9, 1999, and revision received Nov. 23, 1999.